Research Article

Ruxing Shi, Xingsheng Yu, Huiqin Chen*, Yongxing Jiao, Juan Chen, Fei Chen, and Sizhe He

Research on the behaviour and mechanism of void welding based on multiple scales

https://doi.org/10.1515/htmp-2022-0271 received November 05, 2022; accepted February 07, 2023

Abstract: As the core foundation of major national equipment, large forgings have a great influence on the national economic construction, the development of national defence equipment and the development of modern cutting-edge science and technology. In the production of large forgings, welding the internal void of forgings is a technical problem that directly affects the quality of large forgings. In view of the phenomenon of void welding in large forgings, the behaviour and mechanism of void welding were deeply studied based on the stretching test and molecular dynamics simulation, combined with a lot of theoretical analysis. The results show that multi-pass stretching deformation is a kind of plastic deformation process which can eliminate void defects. When the forging ratio reaches 2.2, the void can be welded completely and the tensile strength can be restored to the level of the matrix. With the increase of compression deformation, the stress will increase sharply, especially at the grain boundary. In addition, the main void welding mechanism of 30Cr₂Ni₄MoV steel is the recrystallization and grain growth mechanism. Recrystallization and grain growth are of great significance for promoting the reduction of void volume and realizing metallurgical bonding of the interface.

Ruxing Shi, Xingsheng Yu: Luoyang CITIC-HIC Casting and Forging Co., Ltd., Luoyang, Henan 471003, China; Henan Province Heavy Casting & Forging Technology Center, Luoyang, Henan 471003, China

Yongxing Jiao, Juan Chen, Fei Chen, Sizhe He: School of Materials Science and Engineering, Taiyuan University of Science and Technology, Taiyuan, 030024, China; Shanxi Heavy Casting and Forging Engineering Technology Research Centre, Taiyuan, 030024, China

Keywords: void welding, numerical simulation, physical simulation, molecular dynamics

1 Introduction

The large casting and forging industry is a special and important industry, and its development level is a symbol of measuring a country's comprehensive national strength [1]. The large cast and forged products are the core basic components of electric power, metallurgy, petrochemical, shipbuilding, railway, mining, aerospace, military, engineering and other pieces of equipment. It is the basis of major equipment manufacturing, related to national security and national economic lifeline. Because of the high requirements for the organization and mechanical properties of large forgings, coupled with the extremely high manufacturing costs, forged products require strict control of quality. However, the large size of the ingots used in the manufacture of large forgings, the uneven temperature distribution during the casting process, and the core area of the ingot due to the cooling rate of the diffuse easily produce shrinkage, voids and other void defects [2,3]. These void defects must be eliminated by a reasonable forging process to ensure the production quality of forgings.

The elimination of void defects consists of two parts: void closure and void welding [4]. After the void is closed, the upper and lower surfaces of the void gradually fit together to form a crack, which then requires further plastic deformation or high-temperature insulation to achieve the void weld [5]. The study of the mechanism of void welding during the thermal processing of metals is essential for the improvement of the quality of large forgings. In view of the similarity between void welding and crack repair, a lot of research has been done by scholars at home and abroad on this issue. Han et al. [6] studied the effect of different temperatures and holding times on crack repair using crack prefabrication with 20MnMo steel as the object, analysed the microstructure evolution in the crack repair area, the extent

^{*} Corresponding author: Huiqin Chen, School of Materials Science and Engineering, Taiyuan University of Science and Technology, Taiyuan, 030024, China; Shanxi Heavy Casting and Forging Engineering Technology Research Centre, Taiyuan, 030024, China, e-mail: chen_huiqin@126.com

of recrystallization and grain size changes, and finally, determined the process conditions under which the crack could be repaired; they showed that crack repair is achieved by relying on the atomic motion. Zhang and Sun [7] studied the effect of crack repair by prefabricating artificial cracks. The crack repair mechanism during annealing at 900°C under vacuum conditions was investigated by observing the evolution of cracks during the experiment, showing that crack repair is strongly related to both atomic and lattice diffusion. Gao et al. [8] used carbon steel as the object of study and observed the crack repair process inside the material through rolling deformation, and found that the crack repair is mainly affected by the nucleation and growth of recrystallized grains. The newly grown grains were found to complete the crack repair along both sides of the crack and gradually filled in. Yuan et al. [9] investigated the repair behaviour and grain refinement mechanism of cracks within the material based on compression experiments at different temperatures and found that the recrystallization and growth behaviour of the grains could indeed repair larger size cracks through tissue observation. However, this repair mechanism must be achieved above the recrystallization temperature and cannot explain the crack repair behaviour in deformation if the low temperature does not allow recrystallization to occur. Xin et al. [10] investigated the high-temperature crack repair and tissue evolution in low-carbon steel and found that at 900°C, ferrite was enriched near the crack and crack repair was dominated by diffusion migration of atoms. At 1,000°C, recrystallization occurs near the crack and the crack gap was filled by a large number of fine equiaxed ferrite grains. At 1,200°C, the equiaxed ferrite grains grow into chains and grains grow across the original crack area, and the crack repair was dominated by recrystallization and grain growth to achieve crack healing.

However, the current research mainly stays at the qualitative level, mostly describing the phenomenon of void welding in deformation and the welding process in general, lacking further research on the mechanism;

quantitative research such as judging criteria is still in its infancy, while the research involving large forgings is even less and no unified understanding has been formed. Molecular dynamics (MD) is a molecular simulation method, which relies on Newtonian mechanics to simulate the motion of molecular systems, and it can reveal the nature of some things from a molecular point of view [11,12]. It is rare to combine MD with void welding tests to study the mechanism of void welding.

In this article, physical simulations were carried out to investigate the behaviour of void welding and the welding mechanism of 30Cr₂Ni₄MoV steel under high-temperature plastic deformation conditions. Then, the compression simulation of FeCrNi polycrystals with cracks and interfaces was carried out by MD simulation. The mechanism of void welding was revealed from multiple scales by combining the microstructure evolution of the void welding zone obtained from experiments with the MD simulation results.

2 Materials and methods

2.1 An experimental programme for void welding

It is difficult to achieve complete welding of a void with only a single compression deformation and must be achieved with multi-pass deformation or a single deformation with a high-temperature holding method. Therefore, this work investigated the multi-pass deformation of void welding using wide die heavy blow forging of as-cast 30Cr₂Ni₄MoV ingots.

The size of the test ingot was $150 \, \text{mm} \times 150 \, \text{mm} \times 120 \, \text{mm}$ and a through-hole was drilled in the heart of the original specimen with a diameter of 10 mm. Then, a cylinder of the same diameter as the through-void was placed to plug the through-void and welded to prevent

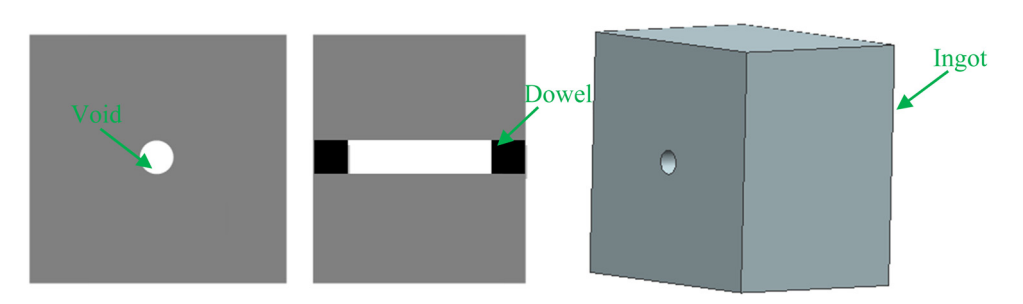


Figure 1: Compressed sample diagram.

DE GRUYTER

oxidation inside the void during heating, as shown in Figure 1. The die used in the drawing is divided into an upper die and a lower die and is symmetrical in size, measuring $200 \text{ mm} \times 200 \text{ mm} \times 90 \text{ mm}$. The anvil to width ratio in the drawing forging is 0.6. After the die is machined, it is mounted on a 500 t hydraulic press for compression experiments. The lower die is fixed after installation, and the upper die moves with the hydraulic press, with the pressing speed set at 4 mm·s^{-1} .

Before the stretching test, the specimens were heated in a heating furnace at a rate of 10°C·min⁻¹ to 1,200°C and the holding time was 5h. After heating, the test was carried out. The deformation temperature used in the stretching was 1,200°C. The original microstructure is shown in Figure 2. The original grain size is mainly coarse grain with an average grain size of 301.41 µm. Different deformation ratios were chosen: 1.8, 2.0 and 2.2. In the stretching process, the workpiece deformation in different passes was shown in Table 1. After stretching, the specimens were rapidly water-cooled to retain their postforging state. The specimens were then sectioned along the direction of compression using a wire cut and sampled at 1/4 (Section I) directly below the die to remove the sample including the void, as shown in Figure 3. After grinding, polishing and etching the small samples, the evolution of the voids was observed by optical microscopy. The etching solution was a saturated picric acid with a small amount of detergent. The etching process was carried out in a 40°C water bath and wiped with alcohol after 3-5 min of etching. In the study of void welding, in addition to observing the change in the microstructure, it is also necessary to test the recovery of tensile properties of the sample at room temperature, which requires the use of a static load tensile experiment. The deformed specimen should be sampled first, and the tensile specimen should ensure that the void repair zone is in the middle part. At the same time, the ingot without the artificial void should be deformed under the

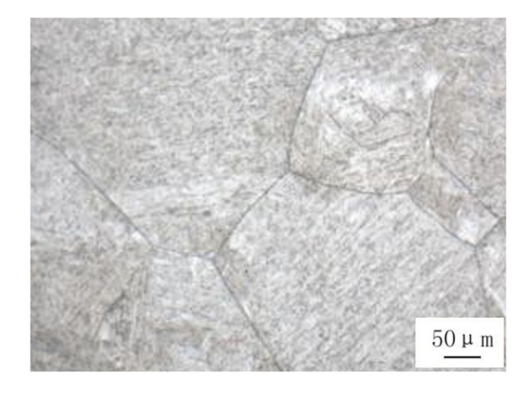


Figure 2: The original microstructure.

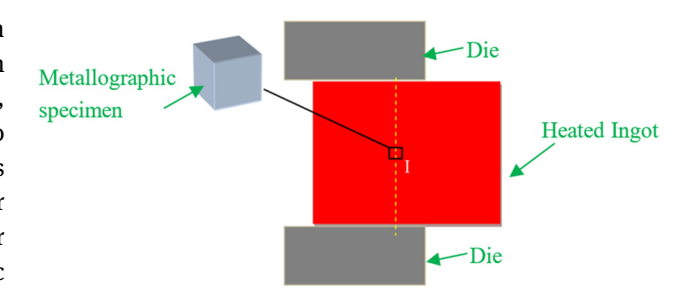


Figure 3: Sampling diagram of the specimen.

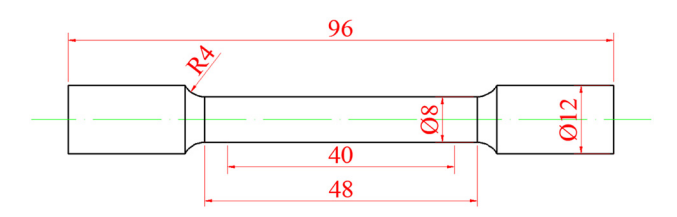


Figure 4: Tensile sample.

same deformation conditions as the ingot with the artificial void. Tensile samples should be taken at the same position as the ingot with the artificial void and then compare with their tensile strengths. The size of the tensile sample is shown in Figure 4.

2.2 MD models

Using Atomsk software, 18 wt% Cr and 9 wt% Ni were added to the FeCrNi polycrystalline austenite sample [13]. The polycrystalline sample had dimensions of $82 \times 82 \times 10 \text{ nm}^3$ and contained 1,094,283 Cr atoms, 788,808 Ni atoms and 3,877,596 Fe atoms with a lattice parameter of 0.35 nm. The sample consisted of 28 different grains. Eight of the complete grains were built around an interface located in the middle of the sample (Figure 5(a)). Another sample considered prefabricated cracks placed in the interface, where two triangular grain boundaries (GBs) on the interface were chosen as the starting ends of the prefabricated cracks (Figure 5(b)). By deleting the atoms, prefabricated cracks with a length of 51 nm and

Table 1: Single-pass deformation in stretching experiments

Forging ratio	First (%)	Second (%)	Third (%)	Fourth (%)
1.8	10.0	20.0	22.2	8.3
2.0	10.0	23.3	24.4	7.9
2.2	15.0	25.3	27.4	8.9

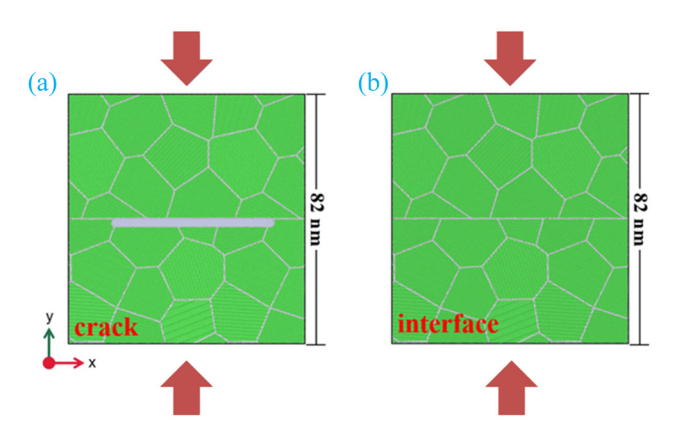


Figure 5: Schematic of the samples with crack and interface loaded under compression and shear stress.

a width (approx. 2.8 nm) of about six times the average width of the GBs appear in the sample, as shown in Figure 5. The simulation process can be divided into two stages: a relaxation and a mechanical loading phase. Before loading, the designed samples were first relaxed to a local energy minimum by a maximum descent algorithm, then equilibrated for 90 ps at a constant temperature of 300 K using an NVT ensemble and a Nosé–Hoover thermostat, followed by an NPT ensemble during compression.

Atomic interactions in FeCrNi samples were described using the embedded atom method potential function, which is designed to describe austenite properties over a large concentration range based on ab initio calculations [14]. This potential has been successfully used to describe dislocation motion [15], the relationship between solute segregation and GB states as well as high-energy collisional cascades and ab initio calculations for FeCrNi alloys [16,17]. In this work, polycrystalline samples were visualized and analysed using OVITO software [18]. The simulations were performed by the large atomic parallel simulator [19].

3 Results and discussion

3.1 Void welding behaviour at a microscopic scale

A saturated picric acid solution was used as an etching solution to study the crack repair mechanism of 30Cr₂Ni₄MoV steel to observe the presence of recrystallized grains in the cracked area. After deformation with a forging ratio of 1.8, the microstructure of the matrix around the void of Section I directly below the die is shown in Figure 6(a) and (b);

where Figure 6(b) is the enlarged view on the right side of Figure 6(a). According to Figure 6(a) and (b), the grain size of the matrix is about 58.01 µm. In addition, there are some recrystallized grains around the void because there are many defects on the boundary of the void, which have high energy, making the atoms easy to diffuse. It is conducive to composition fluctuation, energy fluctuation and structure fluctuation. These factors together provide sufficient conditions for the nucleation and growth of recrystallization [4,10,20]. So, small recrystallized grains appear on the boundary, which plays an important role in void welding. On the left side of Figure 6(a), part of the recrystallized grains around the crack has grown and are connected with the surrounding matrix grains, and the crack begins to appear discontinuous, which is disconnected by the newly formed grains and is no longer continuous. The right side of Figure 6(a) shows the crack morphology near the void. The crack is not flat but distributed along the GB.

Figure 6(c)-(e) shows the void welding of the specimen at Section I of the die when the forging ratio is 2.0, and Figure 6(f) shows the void welding of the specimen when the forging ratio is 2.2. Figure 6(c) and (d) shows the microstructure around the void and the crack morphology after void closure. It can be seen from Figure 6(c) that when the forging ratio increased to 2.0, the original void disappeared and a clear dividing line was left, along which intermittent micropores were distributed linearly. According to Figure 6(d), there are a large number of recrystallized grains arranged along the crack direction around the microvoids, which is caused by the recrystallization behaviour. Figure 6(e) shows the crack morphology. It can be seen from Figure 6(e) that the matrix microstructure is relatively uniform, the original coarse grains have been refined, and the newly generated recrystallized grains have also grown, with an average grain size of 50.15 µm. As can be seen from Figure 6(e), part of the cracks evolved into GBs of the new grains, and the grain grew through the original cracks to make the microstructure of the crack zone gradually identical to the matrix. Moreover, the new grains cut the original void into many short cracks, some short cracks spheroidized to form microvoids, and the short crack after segmentation became significantly smaller. This phenomenon is more pronounced when the forging ratio reaches 2.2, as shown in Figure 6(f). At this point, the microcracks are barely visible. According to the above analysis, the greater the deformation, the higher the degree of recrystallization and the higher the degree of void welding.

In addition to analysing the metallography, it is also necessary to study the recovery of mechanical properties in the study of void welding [21]. The ingots with different forging ratios were sampled and then the tensile test was

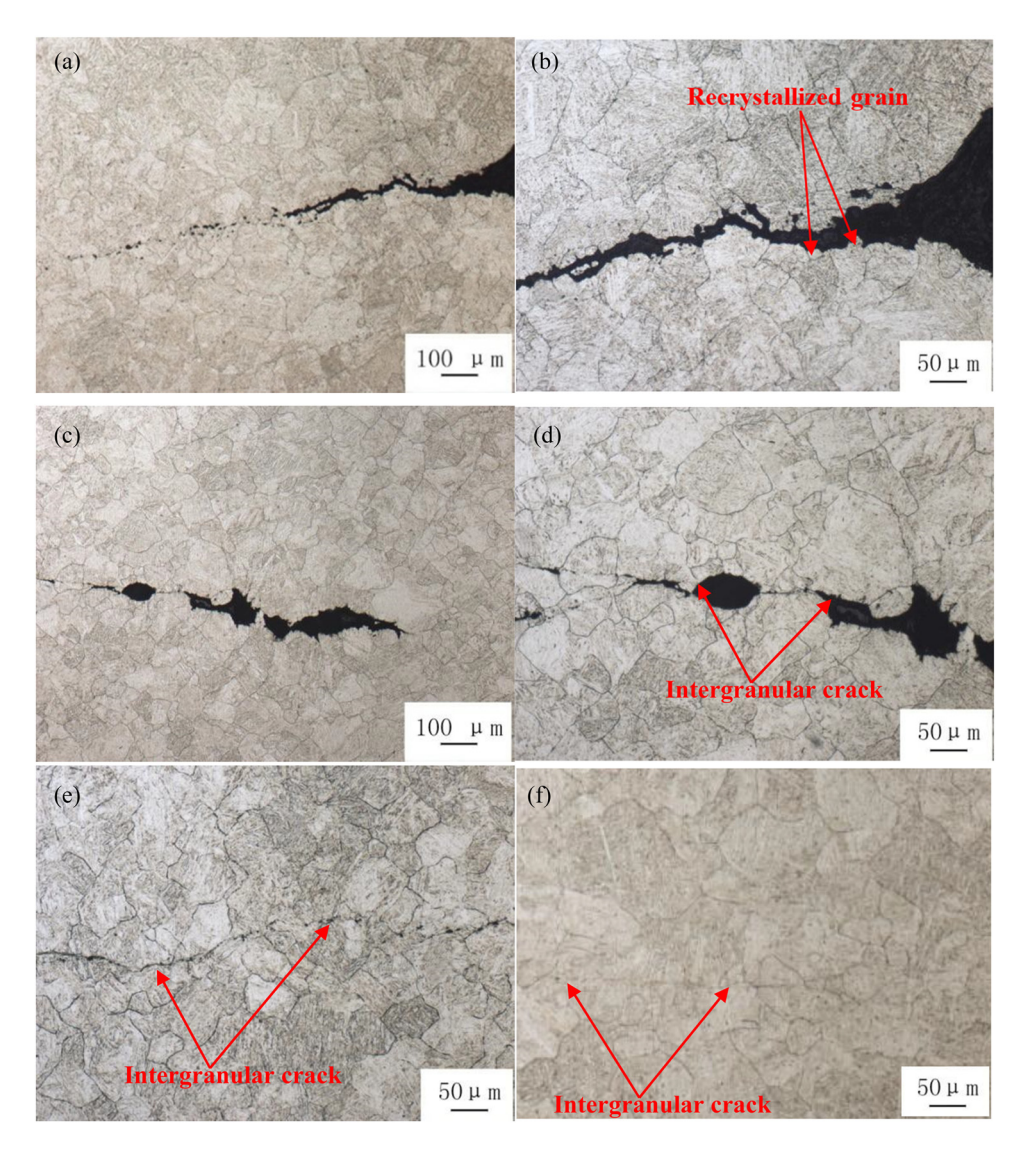


Figure 6: Microstructure evolution during void welding. Forging ratio: (a) and (b) 1.8; (c)-(e) 2.0; and (f) 2.2.

carried out. The recovery of the tensile strength of the material is shown in Figure 6. In the figure, the tensile strength recovery rate of the material is the ratio of the tensile strength of the sample with an internal void to the sample without void after deformation at the same forging ratio. As can be seen from Figure 6, with the increase of the forging ratio, the tensile strength recovery rate gradually increases. For the material with a void in the core, the tensile strength only recovers 42% when the forging ratio is 1.8, which is far different from that of the matrix. When the forging ratio is increased to 2.0, the tensile strength recovery rate reaches 98%. When the forging ratio is 2.2, the tensile strength recovery rate is close to 100%. At this point, the void can be considered completely welded. This is because when the forging ratio

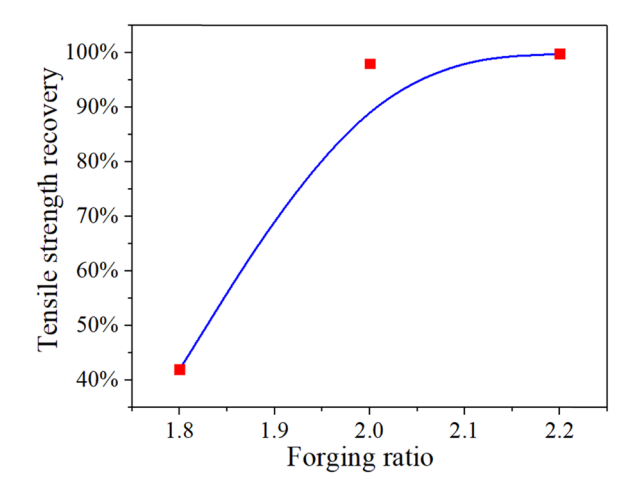


Figure 7: Microstructure evolution during void welding.

6 — Ruxing Shi et al. DE GRUYTER

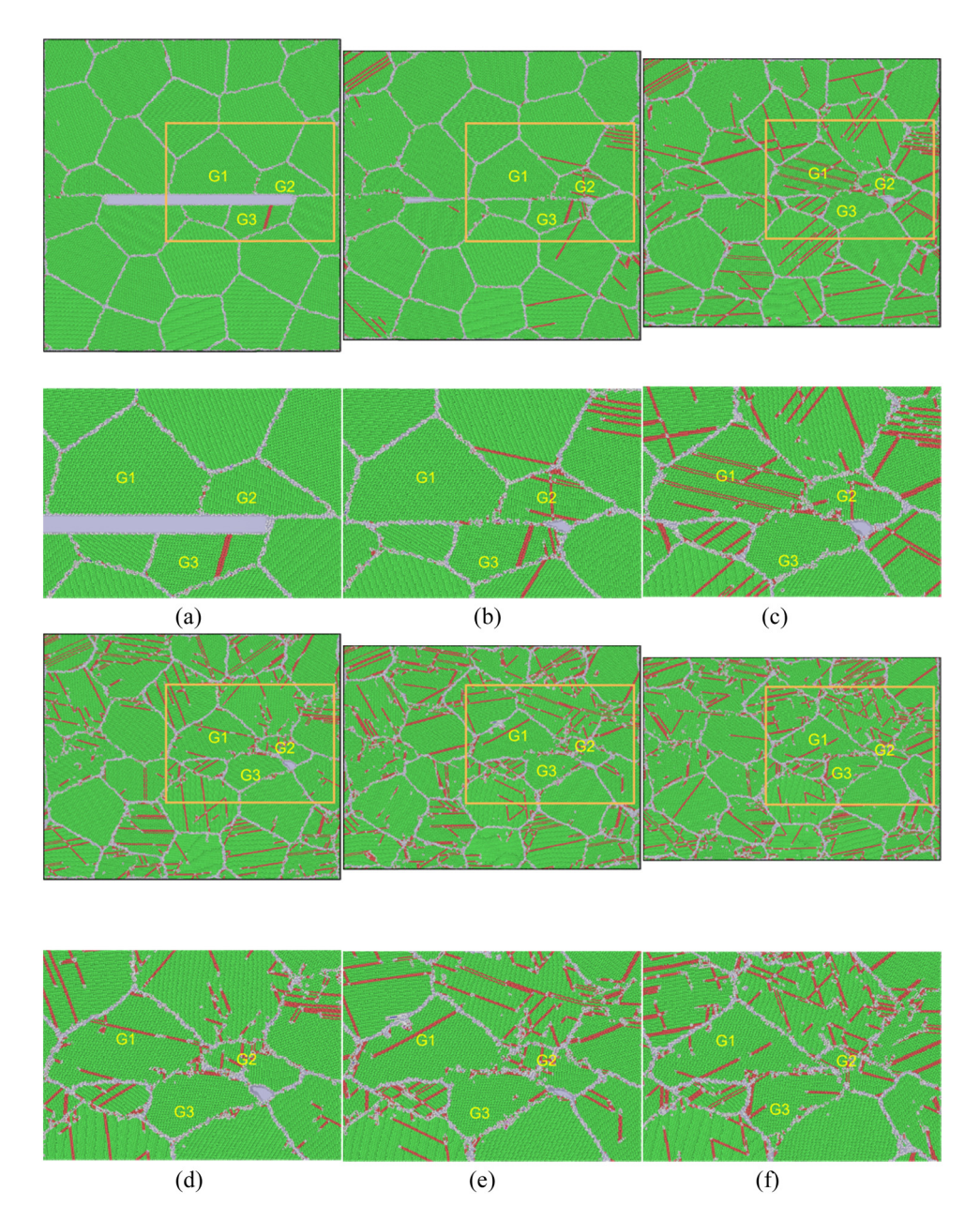


Figure 8: Microstructure evolution of samples with a crack under compressive deformation. Compressive deformation: (a) 0.0%, (b) 5.0%, (c) 10.0%, (d) 15.0%, (e) 20.0% and (f) 25.0%.

is increased to 2.2, the void has been completely welded due to recrystallization and grain growth (Figure 7).

Based on the above analysis, the void welding mechanism of $30 \text{Cr}_2 \text{Ni}_4 \text{MoV}$ steel is mainly recrystallization and grain growth. Recrystallization causes the crack to be quickly healed, grain growth makes the weld zone microstructure uniform, and atomic diffusion provides material sources for recrystallization and grain growth.

3.2 Void welding behaviour at the nanoscale

The evolution of the microstructure of the sample containing the crack during compression is shown in Figure 8. By comparing the atomic configuration of the specimens at the same strain rate it can be found that the upper and lower interfaces in the middle of the crack gradually contact each other when the compressive deformation reaches 5.0%. Voids appear at

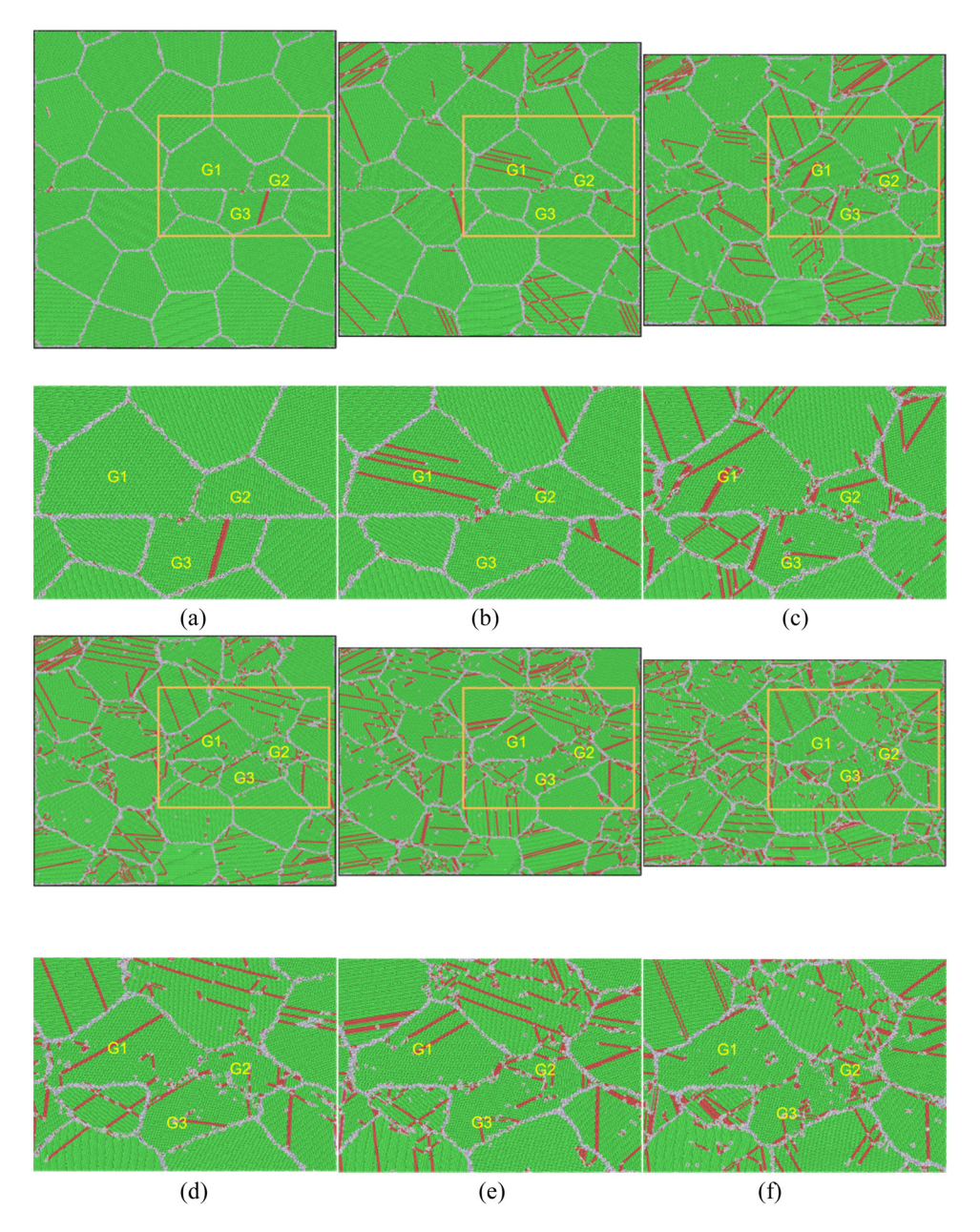


Figure 9: Microstructure evolution of samples containing interface under compressive deformation. Compressive deformation: (a) 0.0%, (b) 5.0%, (c) 10.0%, (d) 15.0%, (e) 20.0% and (f) 25.0%.

the ends of the crack and gradually decrease in size, eventually disappearing as the compressive deformation increases. When the compressive deformation increases to 10.0%, the crack is hardly observable. As the compressive deformation continues to increase, the new relatively straight interface created after crack closure bends due to dislocation-dominated plastic deformation, indicating that the grains have started to grow across the crack.

The evolution of the microstructure of samples containing interfaces during compression is shown in Figure 9.

For samples with interfaces, the original long and straight interface shape becomes jagged as strain accumulates. Some of the smaller grains on either side of the interface continue to cluster with the surrounding larger grains, resulting in grain coarsening. Considering the grains G1, G2 and G3 with the interface as an example, when the compressive deformation reaches 20.0%, the GBs among G1, G2 and G3 start to disappear and the grains gradually fuse. When the compressive deformation reaches 25.0%, the GBs of the three grains begin to disappear and the grains begin to fuse in

8 — Ruxing Shi et al. DE GRUYTER

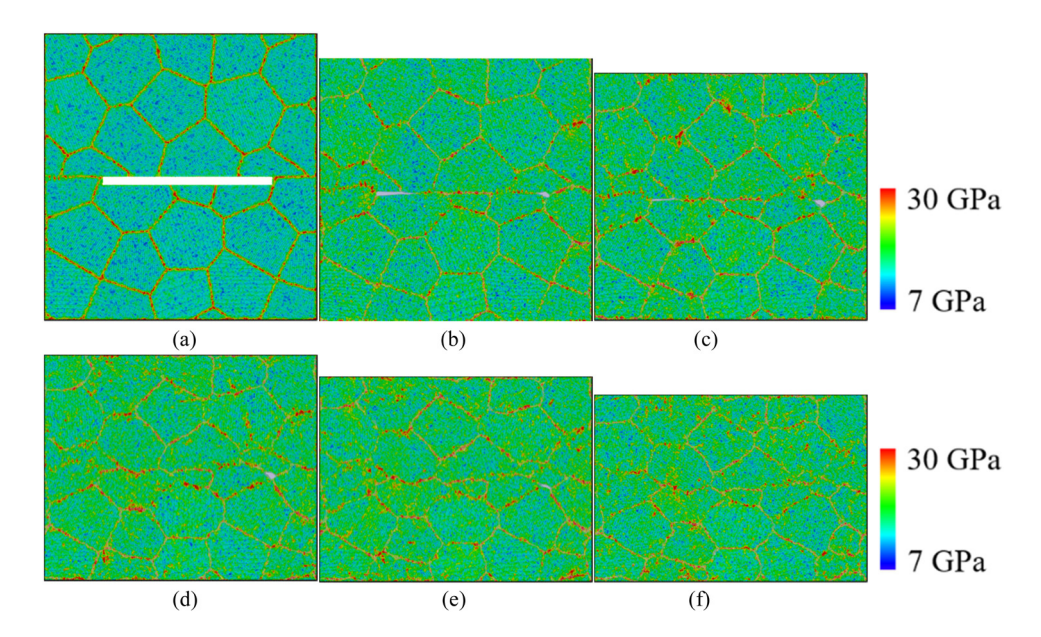


Figure 10: von Mises stress distribution of samples with a crack at different compression deformation. Compressive deformation: (a) 0.0%, (b) 5.0%, (c) 10.0%, (d) 15.0%, (e) 20.0% and (f) 25.0%.

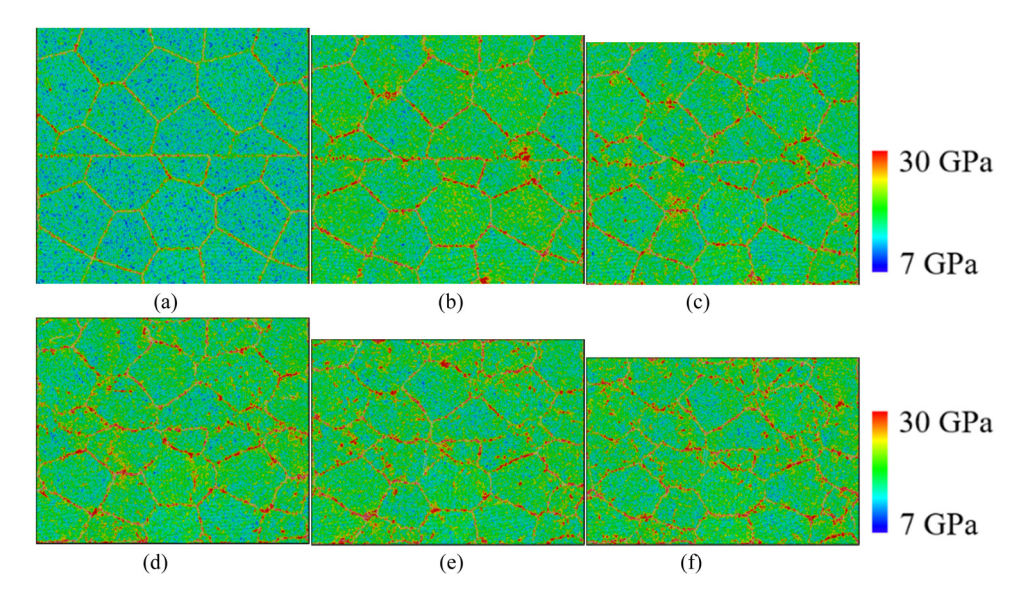


Figure 11: von Mises stress distribution of samples containing interface at different compression deformation. Compressive deformation: (a) 0.0%, (b) 5.0%, (c) 10.0%, (d) 15.0%, (e) 20.0% and (f) 25.0%.

depth. The difference in orientation between the original grains decreases with increasing compressive deformation, indicating that the lattice twists under the action of the compressive deformation, resulting in a slight rotation of the grains and their eventual fusion into one grain.

To further explore the void welding behaviour, von Mises stress analysis is carried out, as shown in Figures 10 and 11. It can be seen that the shear stress values for both samples increase with increasing compressive deformation and that the stress at GBs is significantly higher in the grain interior of the interface containing the sample than in the cracked sample due to the higher stress applied at the same deformation. During the deformation process, the stress is mainly concentrated at the GB, especially in the trigeminal GB region. The stress inside the grain is relatively uniform.

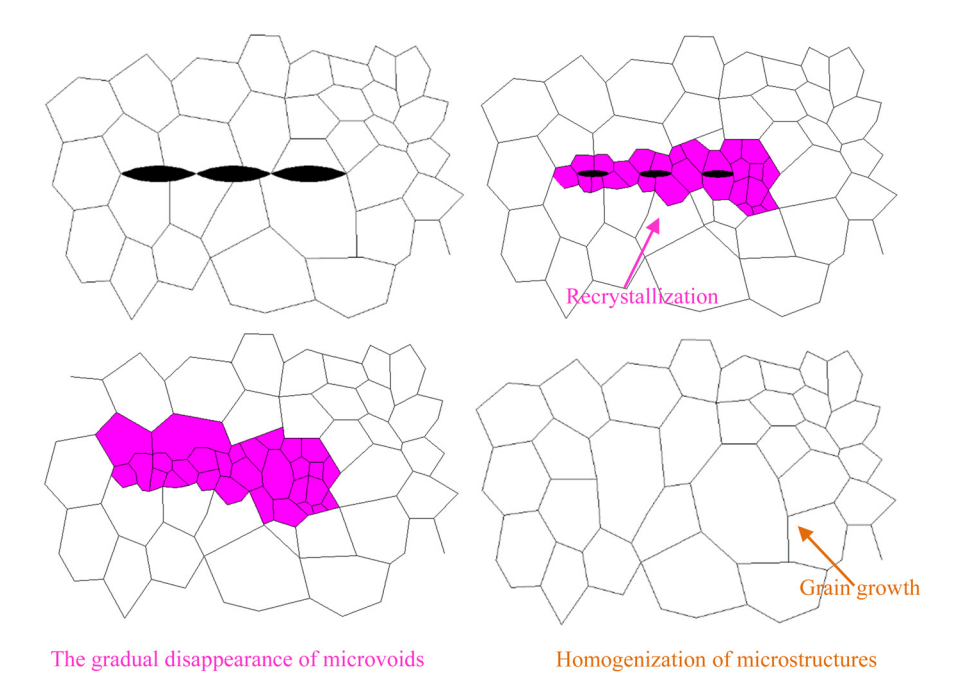


Figure 12: Schematic diagram of the void welding mechanism.

3.3 Void welding mechanism

Figure 12 shows a schematic diagram of the void welding mechanism caused by recrystallization and grain growth of austenite grains. In the process of plastic deformation at high temperatures, recrystallization occurs around the crack. This is because there are many defects and high energy in the crack, where the recrystallized grains are easy to nucleate, providing sufficient conditions for recrystallization and grain growth. In addition, grain growth is also conducive to metallurgical bonding of the interface. The upper and lower free surfaces of the closed void gradually come into contact with each other. With the increase of the compression deformation, the interface of the contact closed void fits, forming smaller microvoids. In the process of continuous plastic deformation, the recrystallized grains on the interface of the crack continue to grow, and the growth of grains makes the microvoids reduce and disappear, finally achieving the effect of homogenization of the microstructure.

In conclusion, from the microstructure evolution of the void welding area obtained from the experimental and MD simulation results and the relevant theoretical analysis, it can be seen that the recrystallization and grain growth mechanism is one of the important mechanisms of void welding. Recrystallization and grain growth in the welding area of the void ensure that the crack is filled continuously. Under the effect of high temperature and high plasticity, the interface realizes metallurgical bonding so that the void is completely welded.

4 Conclusions

Based on stretching tests and MD simulations, the void welding behaviour and mechanism during high-temperature plastic deformation were elucidated based on extensive theoretical analysis. Based on the analysis in this article, the following main conclusions can be drawn:

- (1) It is clear from the stretching tests that multi-pass stretching deformation is a plastic deformation process that can eliminate void defects and achieve void welding completely. When the forging ratio reaches 2.2, the void can be welded completely and the tensile strength can be restored to the level of the matrix.
- (2) The MD simulation shows that the shear stress increases sharply with the compression process. During the deformation process, the stress is mainly concentrated at the GB, especially in the trigeminal GB region. The stress inside the grain is relatively uniform.
- (3) According to the results of the stretching tests and MD simulation, it can be seen that the main welding mechanism of 30Cr₂Ni₄MoV steel is recrystallization and grain growth mechanism, and recrystallization and grain growth are important for promoting the reduction of void volume and achieving metallurgical bonding at the interface.

Funding information: This work was financially sponsored by the "Research Project Supported by Shanxi Scholarship Council of China" (HGKY2019084).

Author contributions: Ruxing Shi: writing – original draft, formal analysis, methodology; Xingsheng Yu: writing – review and editing; Huiqin Chen: project administration; Yongxing Jiao: experiment research; Juan Chen: molecular dynamics analysis; Fei Chen: experiment research; Sizhe He: investigation.

Conflict of interest: The authors declare no conflict of interest.

References

- [1] Zhou, P. and Q. MA. Dynamic recrystallization behavior and constitutive modeling of as-cast 30Cr₂Ni₄MoV steel based on flow curves. *Metals and Materials International*, Vol. 23, No. 2, 2017, pp. 359–368.
- [2] Chen, F., X. D. Zhao, and H. Q. Chen. Void-closure behavior and a new void-evolution model for various stress states. *Materiali* in *Tehnologije*, Vol. 55, No. 1, 2021, pp. 105–113.
- [3] Jiao, Y., C. Zhou, and J. Liu. Void evolution behavior and closure criterion inside large shaft forgings during a forging process. *Materiali in Tehnologije*, Vol. 55, No. 3, 2021, pp. 355–361.
- [4] Chen, F., X. T. Wang, H. Q. Chen, and S. Dang. Behavior and mechanism of void welding under thermal mechanical coupling. *Metals and Materials International*, Vol. 28, 2022, pp. 1751–1762.
- [5] Wang, B., J. Zhang, C. Xiao, W. Song, and S. Wang. Analysis of the evolution behavior of voids during the hot rolling process of medium plates. *Journal of Materials Processing Technology*, Vol. 221, 2015, pp. 121–127.
- [6] Han, J. T., G. Zhao, and Q. C. Cao. Discovery of inner crack recovery and its structure change in 20MnMo steel. *Acta Metallurgica Sinica*, Vol. 32, No. 7, 1996, pp. 723–729.
- [7] Zhang, H. L. and J. Sun. Diffusive healing of intergranular fatigue microcracks in iron dur-ing annealing. *Materials Science and Engineering: A*, Vol. 8, 2004, pp. 171–180.
- [8] Gao, H., Z. Ai, H. Yu, H. Wu, and X. Liu. Analysis of internal crack healing mechanism under rolling deformation. *PLoS One*, Vol. 9, No. 7, 2014, id. e101907.
- [9] Yuan, C. L., Y. X. Zhong, and Q. X. MA. China mechanical engineering. *Tiny Particular Effect in Crack Self-Recovering Processes of Plastic Deformation*, Vol. 1411, 2003, pp. 982–984.

- [10] Xin, R. S., Q. X. MA, and Z. D. Shan. Microstructure evolution of internal crack healing in a low-carbon steel at elevated temperatures. *Journal of Tsinghua University (Natural Science Edition)*, Vol. 55, No. 3, 2015, pp. 304–309.
- [11] Zhang, M., T. XU, M. LI, K. Sun, and L. Fang. Constructing initial nanocrystalline configurations from phase field microstructures enables rational molecular dynamics simulation. Computational Materials Science, Vol. 163, 2019, pp. 162–166.
- [12] Chen, J., J. Shi, Y. Wang, J. Sun, J. Han, K. Sun, et al.

 Nanoindentation and deformation behaviors of silicon covered with amorphous SiO₂: A molecular dynamics study. *RSC Advances*, Vol. 8, 2018, pp. 12597–12607.
- [13] Hirel, P. Atomsk: A tool for manipulating and converting atomic data files. *Computer Physics Communications*, Vol. 197, 2015, pp. 212–219.
- [14] Bonny, G., D. Terentyev, R. C. Pasianot, S. Poncé, and A. Bakaev. Interatomic potential to study plasticity in stainless steels: the FeNiCr model alloy. *Modelling and Simulation in Materials Science and Engineering*, Vol. 19, 2011, id. 085008.
- [15] Fan, Y., W. Wang, Z. Hao, and C. Zhan. Work hardening mechanism based on molecular dynamics simulation in cutting Ni-Fe-Cr series of Ni-based alloy. *Journal of Alloys and Compounds*, Vol. 819, 2020, id. 153331.
- [16] Barr, C. M., G. A. Vetterick, K. A. Unocic, K. Hattar, X. M. Bai, and M. L. Taheri. Aniso-tropic radiation-induced segregation in 316L austenitic stainless steel with grain boundary character. *Acta Materialia*, Vol. 67, 2014, pp. 145–155.
- [17] Béland, L. K., A. Tamm, S. MU, G. D. Samolyuk, Y. N. Osetsky, A. Aabloo, et al. Accurate classical short-range forces for the study of collision cascades in Fe-Ni-Cr. *Computer Physics Communications*, Vol. 219, 2017, pp. 11-19.
- [18] Polak, W. Z. Efficiency in identification of internal structure in simulated monoatomic clusters: Comparison between common neighbor analysis and coordination polyhedron method. Computational Materials Science, Vol. 201, 2022, id. 110882.
- [19] Li, J., L. Dong, H. Xie, W. Meng, X. Zhang, J. Zhang, et al. Molecular dynamics simulation of nanocrack propagation mechanism of polycrystalline titanium under ten-sion deformation in nanoscale. *Materials Today Communications*, Vol. 26, 2021, id. 101837.
- [20] Xin, R. S., Q. X. MA, and W. Q. LI. Effect of heat treatment on microstructure and hardness of internal crack healing in a low carbon steel. *Key Engineering Materials*, Vol. 703, 2017, pp. 3–7.
- [21] He, M., Z. Zheng, F. Shi, D. Guo, and J. Yu. A novel crack healing technique in a low carbon steel by cyclic phase transformation heat treatment: The process and mechanism. *Materials Science & Engineering, A*, Vol. 772, 2020, id. 138712.